

Ultrasonography of the prostate gland and testes in dogs

Mírley Barbosa de Souza

completed a PhD in canine reproduction at the State University of Ceará, and is currently head of diagnostic imaging at Vetclinic, Fortaleza, Brazil.

Lúcia Daniel Machado da Silva

is professor of veterinary obstetrics and animal reproduction at the State University of Ceará, Brazil.

Rachel Moxon

is a canine research associate focusing on canine reproduction and health, and works for Guide Dogs (UK).

Marco Russo

graduated from the University of Naples Federico II, Italy, in 1995. He is currently professor of obstetrics and reproductive diagnostic imaging at the Naples veterinary school.

Gary England

is professor of comparative reproduction at the University of Nottingham. He has a PhD in canine reproduction and is a diplomate of the RCVS, the European College of Animal Reproduction and the American College of Theriogenology.

Mírley Barbosa de Souza, Lúcia Daniel Machado da Silva, Rachel Moxon, Marco Russo, Gary C. W. England

Ultrasonographic imaging is an important diagnostic tool because it allows assessment of the shape, size, position, margination and internal architecture of organs, as well as facilitating the study of vascular supply and vascularisation. Recently, there has been considerable development of B-mode, Doppler and contrast-enhanced ultrasonography for examination of the reproductive tract of dogs, both for studying normal physiology and in the clinical setting. This article describes the practical examination of the canine prostate gland and testes using a variety of ultrasound techniques, and details the normal appearance and blood flow of these organs as well as changes that may be observed with common reproductive disorders.

Imaging the prostate gland

An image of the prostate gland can be achieved by placing the ultrasound transducer on the caudoventral abdomen, adjacent to the prepuce. Most dogs can be examined without sedation while standing or when positioned in dorsal or lateral recumbency. A 7.5 to 10.0 MHz transducer is preferable and imaging is facilitated by the presence of urine within the bladder.

Imaging should always be undertaken in both the transverse and longitudinal planes, while the frontal (dorsal) plane is also useful. When the prostate lies entirely within the pelvis, transrectal imaging can be performed in large dogs but not in small dogs.

B-mode ultrasonography

Normal prostate gland

The prostate is an ovoid-shaped, bilobed gland positioned

at the bladder neck, which encircles the proximal urethra. The normal prostate is positioned within or immediately cranial to the pelvis and is bordered dorsally by the rectum. The gland is smoothly marginated and the parenchyma in entire dogs has a moderate homogenous echogenicity, with a fine- to medium-coarse echotexture (Figs 1, 2).

Prostatic size is often simply assessed by measuring the maximum total prostatic width taken from images in the transverse plane (Fig 2) or by calculating the prostatic volume using the formula for the volume of an ellipse:

$$\blacksquare \text{ Volume} = \text{length} \times \text{width} \times \text{height} \times 0.523$$

Prostatic size varies significantly between dogs (Table 1) and is related to body mass (Fig 3a), although there is substantial variability; the size of the prostate also increases with age in normal dogs (Fig 3b).

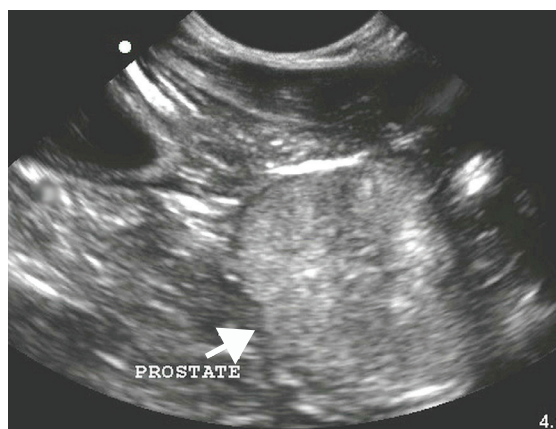


Fig 1: B-mode ultrasound image (longitudinal plane) of a normal prostate gland (arrow). Central hilar echogenic regions are prominent within a moderately echogenic parenchyma

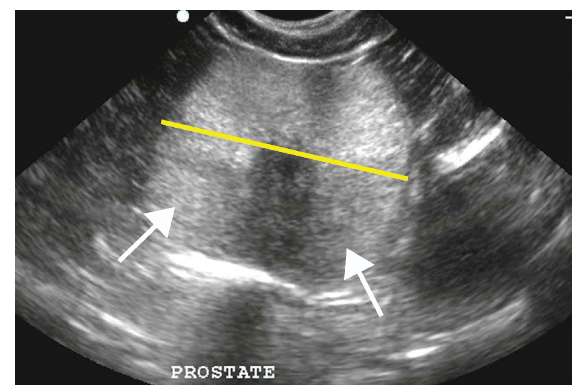


Fig 2: B-mode ultrasound image (transverse plane) of a normal prostate gland. Two symmetrical lobes (arrows) are separated by the urethral region, which appears as a hypoechoic area between the lobes, and there is shadowing distal to the urethra. The yellow line shows the total prostatic width

Companion Animals

Table 1: Approximate prostatic size in entire and neutered dogs of different breeds*

Status	Median prostatic dimensions (range)		
	Length (cm)	Height (cm)	Width (cm)
Entire	2.7 (1.6 to 3.9)	2.4 (0.8 to 3.2)	2.7 (1.2 to 3.6)
Neutered	2.4 (2 to 5.5)	1.5 (1 to 3.5)	1.7 (1.2 to 4.2)

* Adapted from Atalan and others (1999), who examined 60 entire and 17 neutered dogs of different breeds

It is often possible to image the prostatic urethra: in the transverse plane, the mucosal and muscular components may be identified (in the conscious dog, there is not normally urine within the urethra), although more commonly the urethra is recognised simply as a hypoechoic region between the two prostatic lobes (Fig 2).

In normal neutered dogs, the prostate appears smaller compared with entire dogs (Table 1) and after castration the prostatic parenchyma becomes more hypoechoic (Fig 4). The combination of a reduced size and reduced echogenicity often makes it difficult to differentiate the

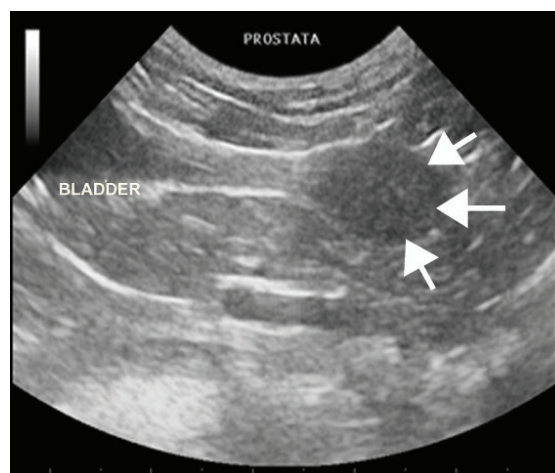


Fig 4: B-mode ultrasound image (longitudinal plane) of the prostate gland (arrows) of a neutered dog. The ellipsoidal-shaped prostate gland appears hypoechoic and is outlined by the thin but echogenic prostatic capsule

gland margins from the periprostatic fat. Prostatic size does not appear to relate to body mass in neutered dogs.

Neutering is not protective of prostatic neoplasia and so imaging of the prostate gland should be considered when clinical signs are appropriate.

Abnormal prostate gland

It is important to recognise that many diseases of the prostate gland may produce a similar ultrasonographic appearance; further diagnostic tests, including the collection of prostatic fluid (by ejaculation or urethral lavage), urinalysis, haematology, fine-needle aspiration (which has a small risk of inducing tumour seeding) or a prostatic biopsy, and further imaging for metastatic disease, are often also warranted.

A common but non-specific finding is prostatomegaly. While B-mode ultrasonography may be useful for the accurate measurement of prostatic size and calculation of prostatic volume, the substantial variation between dogs of similar sizes and the additional effect of age may make this difficult to assess, especially if the changes are small and occur symmetrically. Asymmetrical enlargement is easier to detect and may also result in changes in outline/margination of the gland.

The prostate may succumb to both focal and diffuse parenchyma changes, which may be hyperechoic, hypoechoic or of mixed echogenicity. Again, these changes are non-specific and will require further investigation that might include Doppler or contrast-enhanced ultrasound imaging.

Anechoic cystic structures, which may be single or multiple, parenchymal and/or paraprostatic, may occur in a number of different pathologies.

Benign prostatic hyperplasia

Benign prostatic hyperplasia (BPH) is a spontaneous and age-related condition of intact male dogs and a common incidental finding in older dogs. It does not occur in dogs that have been neutered and many changes seen in cases of BPH will regress in dogs following neutering. In the early stages of the disease, there is commonly symmetrical enlargement of the gland and usually an overall increase of echogenicity, although

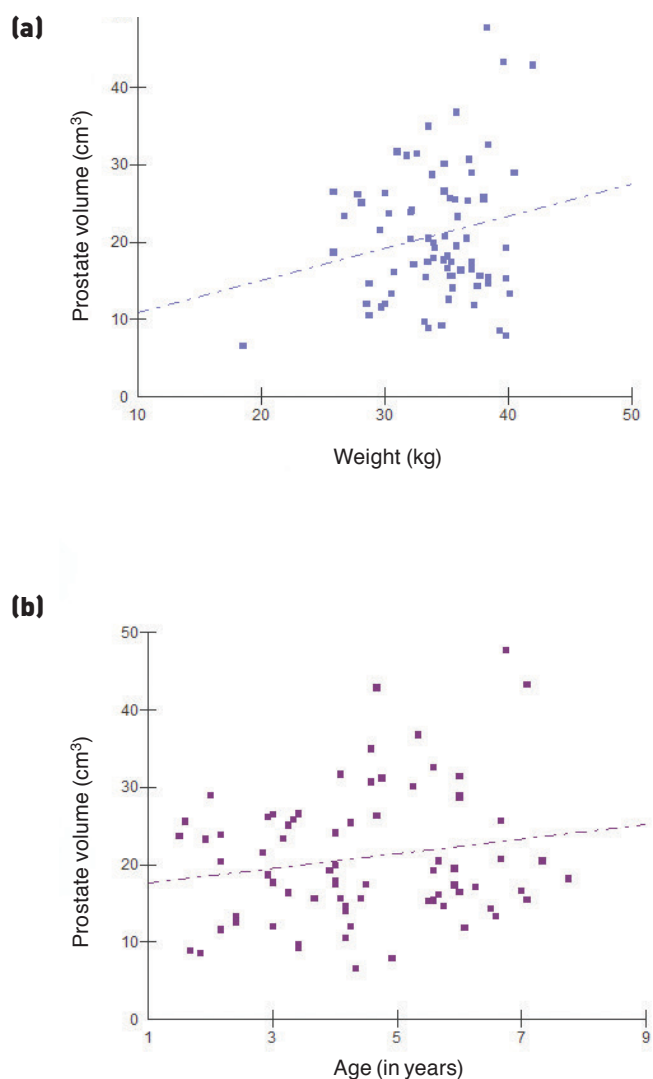


Fig 3: Relationship between (a) prostatic volume and bodyweight, and (b) prostatic volume and age, for 82 clinically normal entire dogs. Prostatic volume increases with age and bodyweight (unpublished observations)

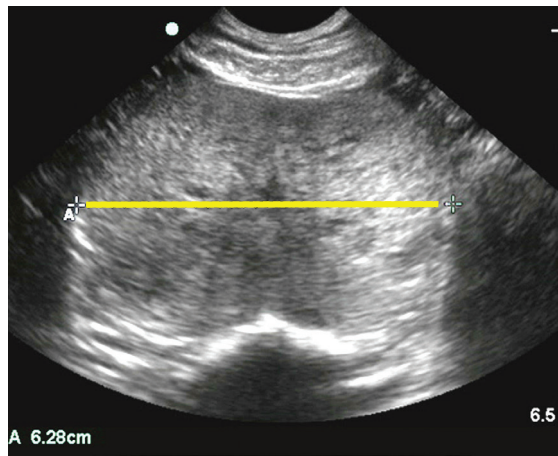


Fig 5: B-mode ultrasound image (transverse plane) of the prostate gland of a three-and-a-half-year-old German shepherd dog with benign prostatic hyperplasia. The gland is enlarged (yellow line shows width) and there is a heterogeneous appearance to the parenchyma. It is also more rounded than normal but the smooth outline is maintained

this is often patchy and not homogenous in appearance (in many cases small 1 to 2 mm diameter anechoic cysts are present). Usually, the normal smooth outline of the prostate is maintained (Fig 5); however, if the enlargement is significant the gland may bulge outwards and lose its typical bilobed appearance. If the condition progresses to a cystic form, the cysts appear as circular to irregular-shaped anechoic areas of variable sizes; commonly, these are up to 2 or 3 cm in diameter. The cysts may increase in size with the progression and severity of the disease, which sometimes results in the gland having a honeycombed appearance.

Cysts

Prostatic cysts may be intraprostatic or paraprostatic. Small intraprostatic cystic lesions are frequently found in asymptomatic dogs and are likely to represent early changes associated with BPH (Fig 6). Dogs with clinical signs of BPH usually have multiple anechoic cysts up to 2 or 3 cm in diameter. In long-standing cases, a small number of these cysts may become very large

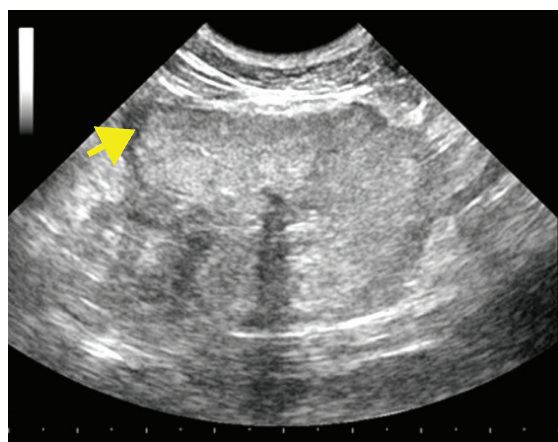


Fig 7: B-mode ultrasound image (transverse plane) of the prostate gland of an intact five-year-old mixed-breed dog with prostatitis. The gland has an irregular outline and a faint hypoechoic rim (yellow arrow), which may be oedema or cellular infiltration. Overall, the parenchyma has an increased echogenicity with a non-homogeneous texture. There is an acoustic shadow distal to the urethra

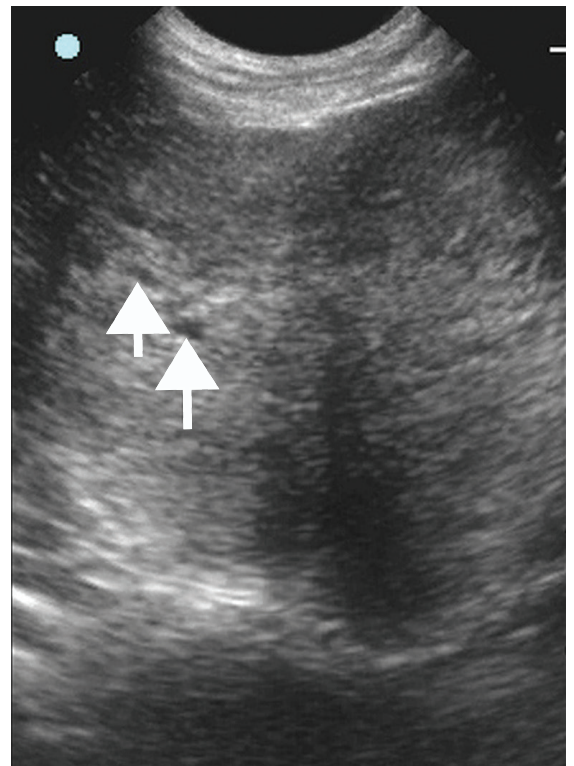


Fig 6: B-mode ultrasound image (transverse plane) of the prostate gland of a six-year-old golden retriever, showing the presence of small anechoic structures (arrows) within the prostatic parenchyma, characterised as clinically insignificant cysts

and protrude from the margin of the prostate gland. Such structures are described as prostatic retention cysts. The large size of these cysts means they may have a similar appearance to a true paraprostatic cyst (fluid distension of a remnant uterus masculinus; that is, persistent Müllerian ducts), and can be difficult to differentiate, although the former is usually associated with other prostatic parenchymal changes typical of BPH. In some cases, the wide base of attachment/origin of the cyst from within the prostate can be detected (in true paraprostatic cysts, the cyst is attached only by a thin stalk-like structure). Large prostatic retention cysts or paraprostatic cysts contain fluid that is anechoic but may become more echogenic and have obvious sediment.

It is not uncommon for internal septation of the cyst cavity to be noted and for the cyst wall to become calcified (these cases have a very similar appearance to a prostatic abscess). Calcification may be present but not evident on ultrasound examination.

Other cystic changes are seen in cases of chronic prostatitis and prostatic abscessation (see later).

Prostatitis

In cases of acute prostatitis, the gland may be enlarged, with a symmetrical or asymmetrical outline. The parenchyma is usually heterogeneous and in acute prostatitis has a hypoechoic appearance, which is followed in more chronic cases by patchy increased echogenicity (Fig 7), with focal echogenic regions. In chronic cases that do not resolve, patchy hypoechoic areas may appear and, with time, coalesce as small fluid-filled microabscesses; these are more irregularly margined than the cysts seen with BPH, and often

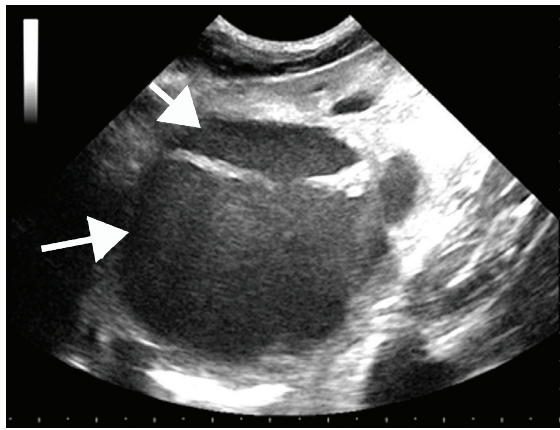


Fig 8: B-mode ultrasound image (longitudinal plane) of the prostate gland of a seven-year-old Italian bracco with prostatic abscessation. The prostate is enlarged and misshapen, with irregularly shaped cavities containing slightly echogenic fluid (arrows), which, on aspiration, contained pus

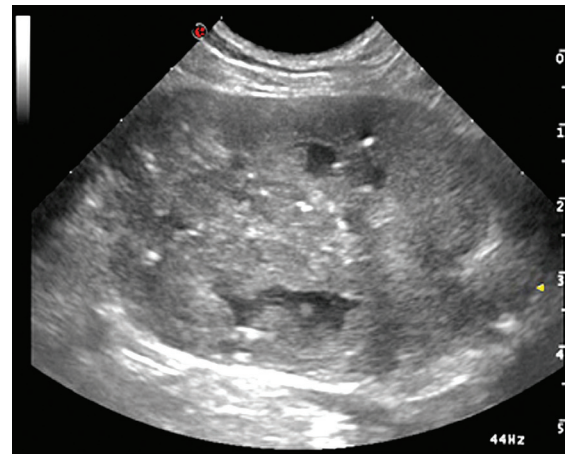


Fig 9: B-mode ultrasound image (longitudinal plane) of the prostate gland of a nine-year-old neutered beagle with a prostatic adenocarcinoma. The gland has an irregular margin and the parenchymal echotexture is heterogeneous with scattered echogenic foci and irregular hypoechoic lesions

contain particulate material or hypoechoic fluid. Abscess cavities may increase in size (Fig 8) and, as a larger lumen forms, the abscess wall may become calcified. Occasionally, prostatic abscesses contain gas, which appears as scattered hyperechoic foci associated with reverberation artefacts. There may also be a low-volume local peritoneal effusion and mesenteric lymph node enlargement.

Neoplasia

Prostatic neoplasia has a variable B-mode ultrasonographic appearance in both entire and neutered dogs. Focal hypoechoic lesions are often seen in the early stages of the disease and can be difficult to differentiate from other pathology, including the patchy appearance seen in cases of BPH. At a later stage, the parenchymal changes are often diffuse, the gland is not symmetrical and the gland margin becomes irregular. There is often a markedly hyperechoic heterogeneous parenchyma, with frequent irregular anechoic regions and zones of calcification creating acoustic shadowing (Fig 9).

Neoplasia is often locally aggressive, and medial iliac lymph node enlargement may be prominent in advanced cases. Common metastatic sites are the liver and spleen, as well as the lung and bone.

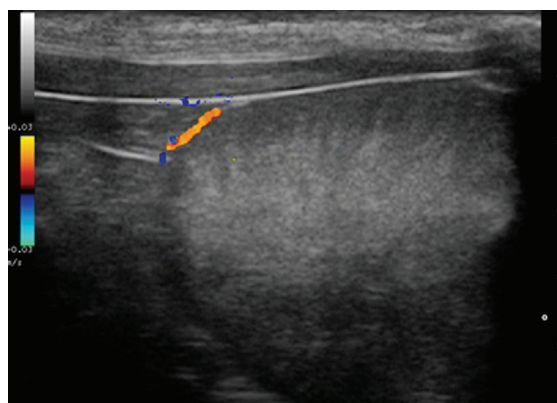


Fig 10: Colour Doppler ultrasound image (longitudinal plane) of the prostate gland of an entire five-year-old male dog. The dorsal prostatic artery can be seen running close to the prostatic capsule

Doppler ultrasonography

Doppler ultrasound techniques involve the simultaneous use of grey-scale ultrasound and either colour Doppler or pulsed-wave (PW) Doppler. With colour Doppler, the direction of movement within specific regions of interest is displayed as a colour superimposed over the grey-scale image; this can be used to locate a vessel and to look at perfusion within an organ. With PW Doppler, the velocity of flow is measured within a specific window and displayed graphically as velocity versus time.

When Doppler techniques are used, it is important to consider the angle of the ultrasound beam, which should be preferably less than 60° away from the direction of flow to ensure an accurate velocity measurement. PW Doppler graphs display velocity of flow within arteries that can easily be interpreted as systole and diastole. By measuring the velocity at the peak of systole (peak systolic velocity [PSV]) and at the end of diastole (end diastolic velocity [EDV]), the downstream resistance and pulsatility can be calculated. From these, the resistance index (RI) and pulsatility index (PI) can be obtained, which are both useful for investigating organ perfusion:

- $RI = (PSV - EDV)/PSV$
- $PI = (PSV - EDV)/M$ (where M is the mean of PSV and EDV).

Normal prostatic arterial blood supply

The two lobes of the dog's prostate gland each have an independent vascular supply. The prostatic artery has an anatomically variable origin, but commonly arises from the internal pudendal artery.

For each lobe, various vessels can be identified in the following regions:

- Cranial;
- Dorsal and ventral subcapsular (also called lateral by some authors);
- Caudal;
- Parenchymal (Figs 10, 11).

Tortuosity of the prostatic veins results in blood flow only being detected in short segments of the relevant vein.

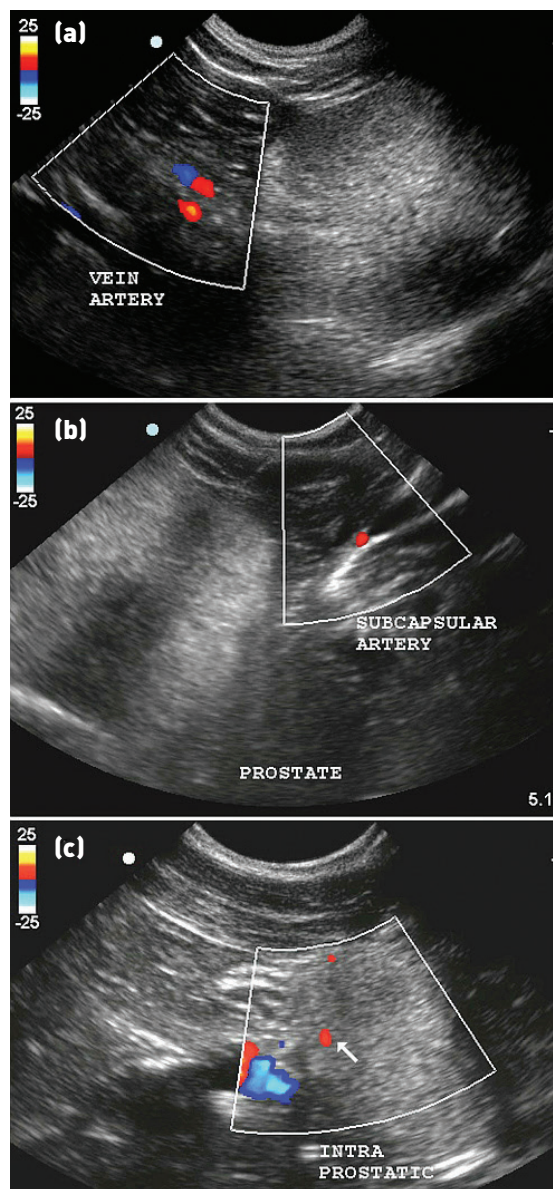


Fig 11: Colour Doppler ultrasound images of the prostatic artery in (a) the cranial, (b) the subcapsular and (c) the parenchymal (intraprostatic) regions

Colour Doppler ultrasonography is useful for identifying the location of the prostatic arterial supply and vessels may be imaged in the transverse or longitudinal plane. Flow characteristics vary according to the region of the prostate artery. PW Doppler shows that the cranial (Fig 12a) and caudal arteries have a high resistance to flow with a biphasic pattern – a sharp narrow systolic peak and low antegrade diastolic flow – which is typical of many normal small arteries. The parenchymal arteries have low velocities, with a monophasic flow

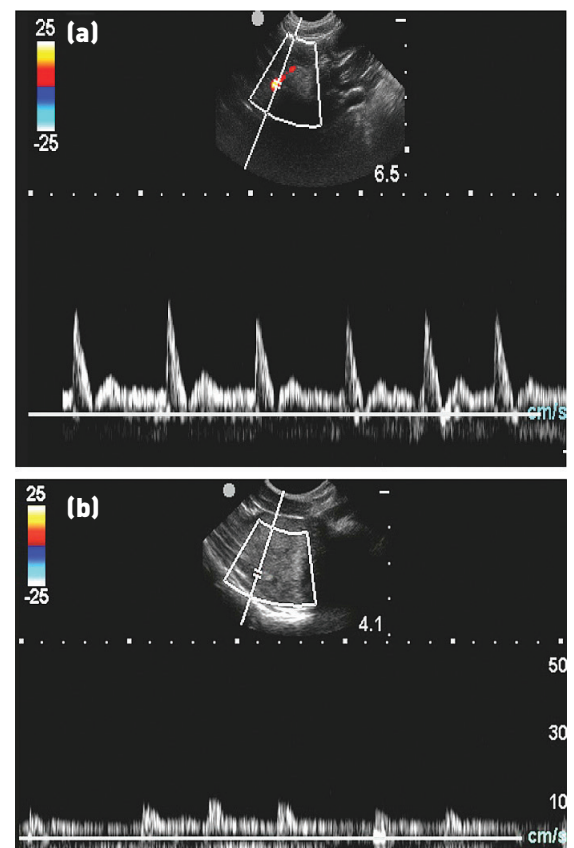


Fig 12: Pulsed-wave Doppler ultrasound images of the prostatic artery in (a) the cranial and (b) the parenchymal (intraprostatic) regions, showing the differences in waveform between the regions

pattern (Freitas and others 2015) (Fig 12b). The velocity decreases between the cranial prostatic artery and the parenchymal prostatic artery.

In normal prostate glands, the RI and PI are low and differ between different regions of the artery (Table 2).

Abnormal prostatic arterial blood supply

Benign prostatic hyperplasia

Measurement of prostatic artery blood flow using PW Doppler is a recent development in the field of small animal reproduction and, at the time of writing, few studies have been published. Nevertheless, it is clear that dogs with BPH frequently show increased PSV and EDV compared with normal dogs (Fig 13). Interestingly, there does not appear to be any change of RI in dogs with BPH.

Neoplasia

In cases of prostatic neoplasia, it may be possible to detect increased blood flow to the gland. However, microvascularisation of prostatic tumours is better visualised using colour and contrast-enhanced ultrasonography.

While, at the time of writing, there are few studies detailing the relationship between prostatic artery blood velocity measured using PW Doppler and disease, it is clear that colour Doppler can be a particularly useful technique to highlight lesions within the prostate gland (Fig 14). In such cases, increased vascularisation within a lesion can be detected readily or there may be an increased vascular supply around a focal lesion. These changes may be useful

Table 2: Approximate Doppler ultrasound measurements of normal prostatic blood flow, according to the region of the artery*

Parameter	Region			
	Cranial	Subcapsular	Parenchymal	Caudal
PSV (cm/second)	25.5	22.0	15.5	23.5
EDV (cm/second)	4.3	6.2	6.7	4.2
RI	0.8	0.7	0.6	0.8
PI	2.5	1.5	0.9	2.3

* Adapted from Freitas and others (2015)

EDV End diastolic velocity, PI Pulsatility index, PSV Peak systolic velocity, RI Resistance index

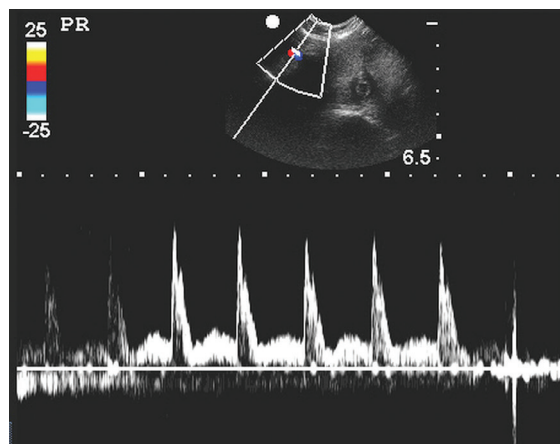


Fig 13: Pulsed-wave Doppler ultrasound image of the prostate gland of a six-year-old golden retriever dog with benign prostatic hyperplasia. Waveforms from the cranial prostatic artery show an increased peak systolic velocity

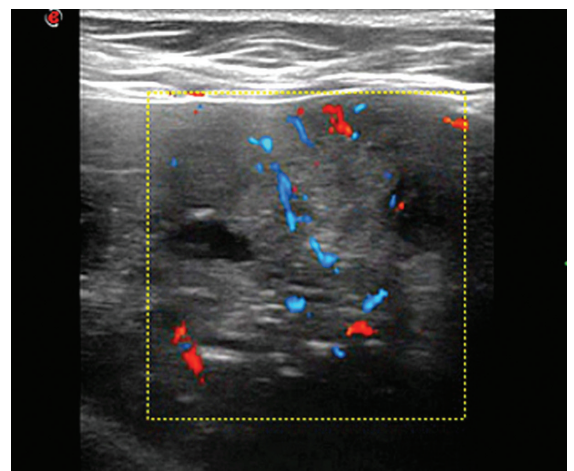


Fig 14: Colour Doppler ultrasound image of a prostatic neoplasm showing irregular increased vascularisation of the entire prostate gland

for documenting the location of a lesion for ultrasound-guided fine-needle aspiration or biopsy. Unfortunately, colour-Doppler ultrasonography cannot currently distinguish between benign and malignant focal lesions.

Contrast-enhanced ultrasonography

Contrast-enhanced ultrasonography (CEUS) is a relatively new technique whereby microbubbles (of gases with high molecular weight and low solubility in water) are injected intravascularly such that the arterial supply, vascular bed and venous drainage can be accurately imaged, generally using a low frequency transducer. Harmonic imaging technology is also helpful but may not be available on all ultrasound machines.

Second-generation contrast agents such as sulfur hexafluoride (SonoVue) are often used and must be matched by an ultrasound beam of appropriate frequency. Images can be directly observed and show vascular detail, or may be subject to quantitative analysis of specific regions of interest using commercial software, allowing the assessment of peak flow, time to reach peak flow, persistence within the vascular bed and time for complete clearance of the contrast media.

Normal prostate gland

After injection of the contrast agent, the prostatic arteries become opaque and are clearly defined from the surrounding tissue. The subcapsular arteries (also called lateral arteries) can be imaged entering the dorsolateral surface of the prostate and have a dorsal

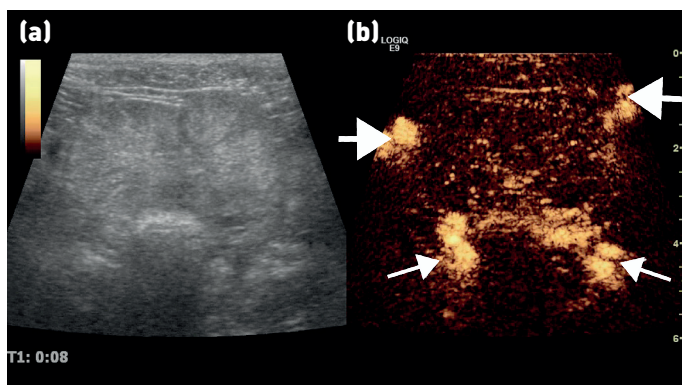


Fig 15: (a) B-mode ultrasound image (transverse plane) and (b) the corresponding contrast-enhanced ultrasound image of a normal prostate gland. The latter image was taken early during the wash-in arterial phase, eight seconds after injection of the contrast material, and shows the dorsal (large arrows) and ventral (small arrows) subcapsular arterial supply

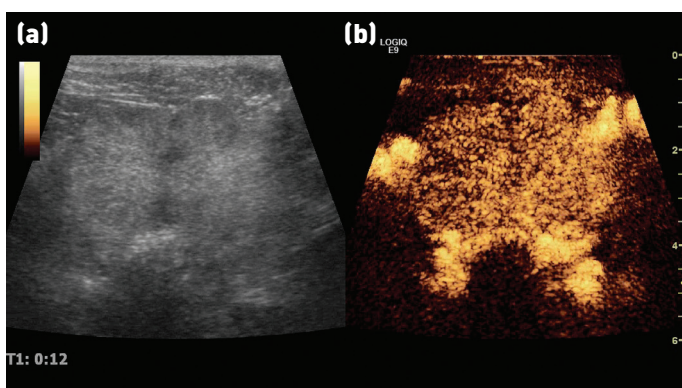


Fig 16: (a) B-mode ultrasound image (transverse plane) and (b) the corresponding contrast-enhanced ultrasound image of a normal prostate gland. The latter image was taken 12 seconds after injection of the contrast material and shows a homogeneous enhancement throughout the prostatic parenchyma. The dorsal and ventral subcapsular arteries remain prominent (compare with Fig 15)

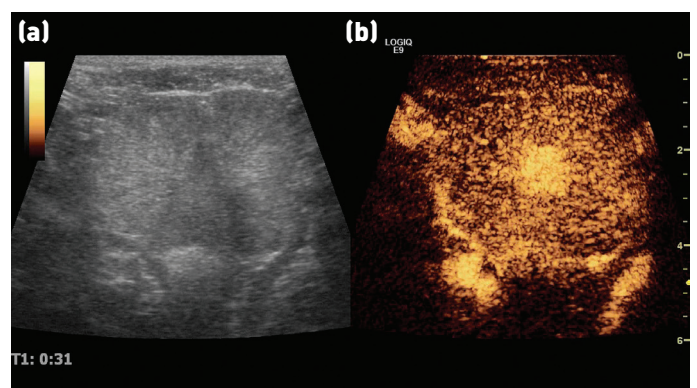


Fig 17: (a) B-mode ultrasound image (transverse plane) and (b) the corresponding contrast-enhanced ultrasound image of a normal prostate gland. The latter image was taken 31 seconds after injection of the contrast material and shows the wash-out phase of the prostatic parenchyma and persistence of the contrast within the urethral mucosa and submucosa

and ventral component. These arteries branch into many small parenchymal arteries, which have a diffuse symmetrical pattern directed medially towards the urethra (Fig 15). Then, during the vascular bed phase, there is increased echogenicity/enhancement of the prostatic parenchyma that is normally homogenous (Fig 16), except for the prostatic capsule, which becomes more echogenic. Finally, during the wash-out phase, the contrast agent is gradually cleared from the parenchyma (Fig 17).

Prostatic veins are also highlighted but have a lower echogenicity compared to the arteries because persistence within the vascular bed results in a longer wash-out than wash-in period.

CEUS offers advantages over Doppler ultrasonography in that prostatic artery branches and parenchymal perfusion are readily observed and can be measured using quantitative methods. Reliable data are available regarding the use of CEUS in normal anaesthetised dogs using standard protocols for administration of the contrast agent (Table 3) (Russo and others 2009, Bigliardi and Ferrari 2011, Vignoli and others 2011); however, more work is needed to document variations in perfusion kinetics and to establish more rapid protocols that can be applied to conscious dogs.

Abnormal prostate gland

Neoplasia

CEUS has the ability to document parenchymal perfusion that might be able to highlight focal lesions and possibly differentiate malignant from benign lesions.

Prostatic tumours can be detected with CEUS and there are trends in perfusion parameters between tumour types (Table 4). For example, values for peak perfusion intensity and the time to reach peak intensity are higher in prostatic carcinomas than in leiomyosarcomas. In addition, different features during the wash-in and wash-out phases can be observed. For example, in cases of prostatic carcinoma, there is hyperperfusion of the

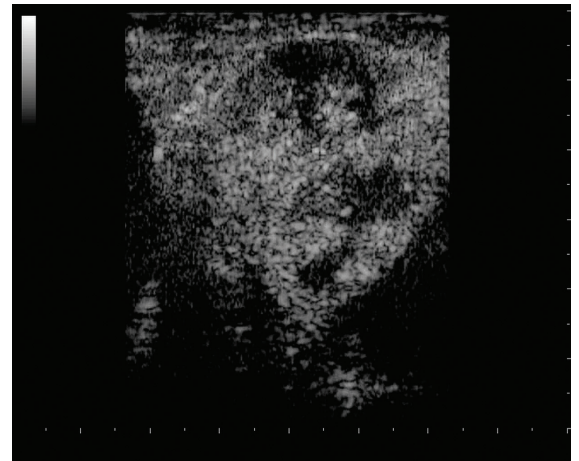


Fig 18: Contrast-enhanced ultrasound image of the prostate gland of a six-year-old Jack Russell terrier diagnosed with a prostatic leiomyosarcoma. The image was taken late in the wash-in phase, 33 seconds after the contrast material had been injected. A non-homogeneous enhancement is present and seen as a hypoechoic lesion compared with the surrounding tissue

tumour during the wash-in phase and hypoechoicity during the wash-out phase when compared to normal dogs. Leiomyosarcomas can be characterised in all phases by a homogenous anechoic non-perfused area surrounded by highly vascularised parenchyma (Fig 18).

Imaging the testes

Ultrasonographic examination of the testes allows the detection of focal and diffuse abnormalities of testicular tissue. It should be performed whenever there is a clinical concern of testicular pathology and may also be used for the routine evaluation of male animals for infertility investigations, in breeding soundness evaluations and to locate testes that are not present within the scrotum.

Ultrasound images can be achieved in the non-sedated dog in lateral recumbency or in the standing position. Clipping of the scrotal hair should be avoided as it is commonly followed by excessive licking and subsequent development of scrotal dermatitis. Instead, copious amounts of ultrasound gel should be used. The testes are imaged in the longitudinal, transverse and dorsal planes.

B-mode ultrasonography

Normal testes

The testicular parenchyma has a hypoechoic background texture overlaid by a homogenous, medium echogenicity, stippled appearance. The parietal and visceral tunics appear as a hyperechoic peripheral echogenic capsule. The mediastinum testis appears as a hyperechoic central line when imaged in the longitudinal plane and as a central circular focal echogenic 'spot' when imaged in the transverse plane (Fig 19). In prepubertal dogs, the echogenicity of the testes is more hypoechoic than in adult dogs, and the mediastinum testis can be identified easily.

There are usually no differences in echogenicity between the right and left testis; however, differences in testicular volume between both testes have been seen in some

Table 3: Quantitative parameters of contrast-enhanced ultrasonography for normal prostate perfusion in anaesthetised dogs*

Parameter	Normal range
Peak perfusion intensity (per cent)	15.5 to 17.6
Time to reach peak intensity (seconds)	29.9 to 37.5
Wash-in phase (seconds)	10 to 15

* Adapted from Russo and others (2012)

Table 4: Perfusion values of quantitative contrast-enhanced prostatic ultrasonography in dogs with benign and malignant lesions*

Parameter	Type of lesion	
	Benign	Malignant
Peak perfusion intensity (per cent)	14.2 to 16.9	14.1 to 23.7
Time to reach peak intensity (seconds)	25.9 to 31.9	26.9 to 41.3

* Adapted from Vignoli and others (2011), who examined 21 dogs with benign lesions (including benign prostatic hyperplasia, mixed benign pathology and prostatitis) and five dogs with malignant lesions

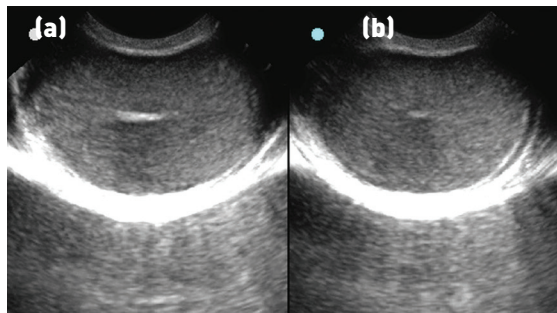


Fig 19: B-mode ultrasound image of a normal testis in (a) the longitudinal and (b) the transverse planes. The mediastinum testis appears as a hyperechoic line in the longitudinal plane and a small central hyperechoic region in the transverse plane

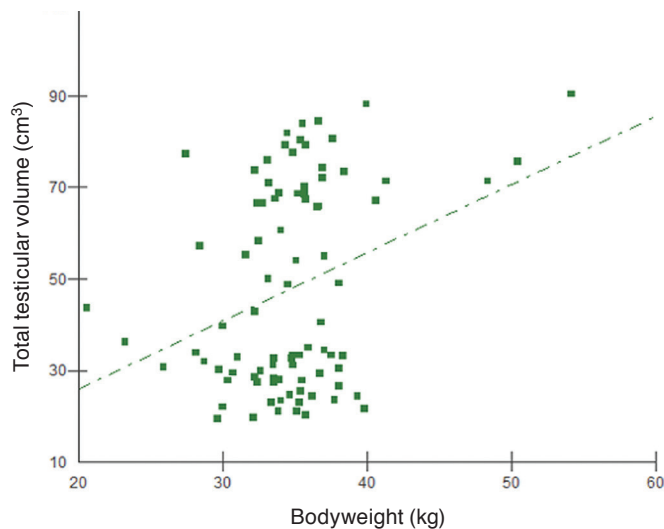


Fig 20: Relationship between total testicular volume (measured using ultrasonography) and bodyweight for 86 normal dogs (unpublished observations)

studies. Testicular volume can be calculated accurately using the formula:

$$\blacksquare \text{ Volume} = \text{length} \times \text{width} \times \text{height} \times 0.5236$$

A number of studies have demonstrated a positive association between testicular volume and canine bodyweight (Fig 20). Mantziaras and others (2014) observed a significant age-related trend of increasing testicular dimensions, which peaked at six years of age and then subsequently decreased.

The epididymis can be identified as a circular and moderately hypoechoic structure (relative to testicular parenchyma), running along the dorsolateral aspect of the testis. The tail of the epididymis can be consistently visualised in the dorsal imaging plane caudal to the testis; it is less echogenic than testicular parenchyma (Fig 21). Measurements of epididymal diameter for all breeds range from 0.6 to 1.3 cm (mean 0.88 [0.20] cm) for the tail; 0.4 to 0.8 cm (mean 0.67 [0.16] cm) for the head; and 0.2 to 0.7 cm (mean 0.39 [0.17] cm) for the body (Pugh and others 1990).

Abnormal testes

Ultrasound may be used to investigate dogs with poor semen quality as well as for a wide variety of testicular abnormalities, including neoplasia, inflammatory disease, testicular trauma and atrophy.

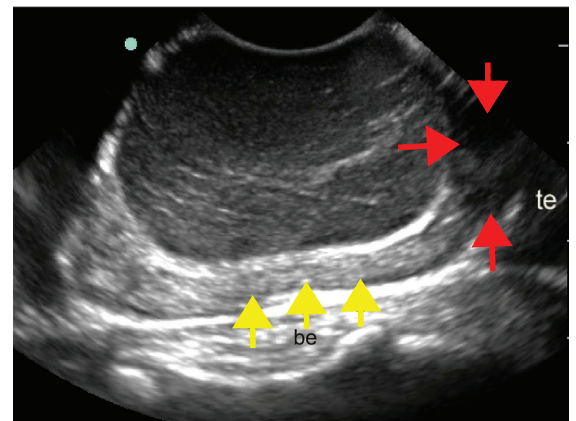


Fig 21: B-mode ultrasound image (longitudinal plane) of a normal testis. The epididymal body runs alongside the dorsal surface of the testis (yellow arrows) (which appears ventral in this image because the transducer is placed on the ventral surface of the testis) and the hypoechoic epididymal tail is located caudally (red arrows)

Testicular appearance and semen quality

A small number of reports document a positive correlation between testicular width and daily sperm output, and a positive correlation between total testicular volume and total sperm concentration in the ejaculate of normal dogs. However, dogs with an abnormal quality of semen may have testicular volumes within the normal range. Nevertheless, changes in parenchymal appearance may be detected using ultrasonography; dogs with poor semen quality have lower parenchymal echogenicity and lower homogeneity (ie, dogs with poorer semen quality have testes that are more hypoechoic and less homogenous than those in normal dogs).

Azoospermic dogs do not always show changes in testicular volume or echogenicity.

Neoplasia

Testicular tumours are the second most common tumour affecting male dogs. They may be benign or malignant and may or may not be endocrinologically active. While B-mode ultrasonography is exceptionally useful for the detection of testicular tumours (Fig 22), the ultrasonographic appearance of the lesions varies and is not specific to the type of tumour. Testicular tumours can range from circumscribed small nodules to large complex masses with a heterogeneous echopattern and disruption of normal anatomy. Sertoli cell tumours and seminomas are usually large with mixed echogenicity, which sometimes results in generalised testicular enlargement. Interstitial cell tumours may appear as well-defined focal hypoechoic lesions. However, areas of haemorrhage and necrosis may occur with all types of tumour and appear ultrasonographically as disorganised hyperechoic and hypoechoic regions.

Other findings that can be associated with testicular neoplasia are areas of calcification within the testicular parenchyma that appear as hyperechoic foci producing acoustic shadowing.

Inflammatory disease

Inflammatory disorders have variable ultrasonographic characteristics, ranging from irregular and often poorly defined anechoic areas to a diffuse, patchy, hypoechoic echopattern (Fig 23).

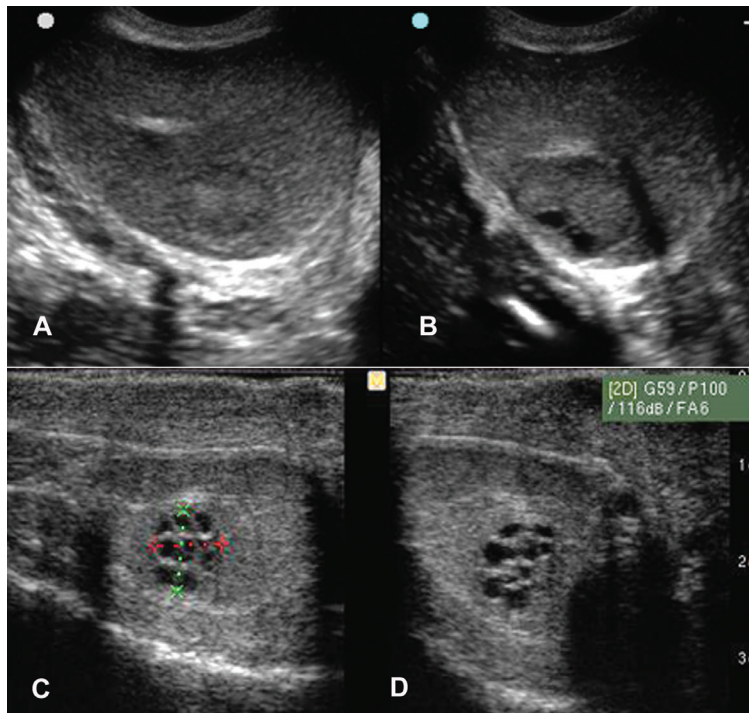


Fig 22: B-mode ultrasound images of two different Leydig cell tumours. (a) Longitudinal and (b) transverse plane images of the testis of a seven-year-old Labrador retriever, showing a circumscribed hypoechoic mass with two small anechoic regions. An acoustic shadow from the mediastinum testis can be seen in (b). (c) Longitudinal and (d) transverse plane images of the testis of a four-year-old German shepherd dog, showing a well-circumscribed mass with multiple anechoic cavities

Orchitis often occurs together with epididymitis in dogs. It may arise following haematogenous spread, bacterial colonisation (eg, from urinary tract or prostatic inflammation) or scrotal trauma. In long-standing cases, abscesses may form. The testis and epididymis are usually enlarged, and fluid may accumulate between the visceral and parietal tunic within the scrotum.

Testicular degeneration

Testicular degeneration (also called testicular atrophy or acquired gonadal dysfunction) is not uncommon, although the cause is often unknown because the initiating testicular insult (eg, raised scrotal temperature, exposure to toxins or endocrine disturbances) probably occurred many months previously. The condition is commonly bilateral but may be unilateral. In the early stages of disease, the testes have focal or regional areas of increased echogenicity and there are often hyperechoic foci or significant hyperechoic lines that radiate outwards to the periphery of the testis (Fig 24). Later in the disease process, the volume of the testes

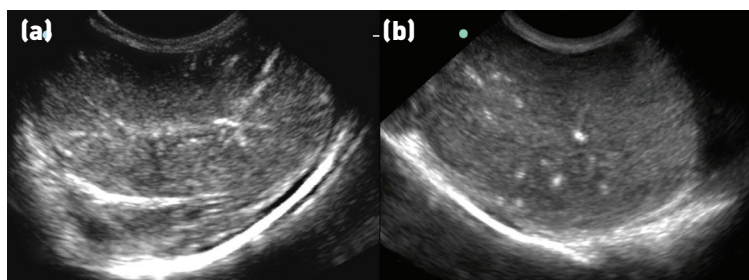


Fig 24: (a) Longitudinal and (b) transverse B-mode ultrasound images of the testis of a three-year-old German shepherd dog with testicular degeneration. There is gross distortion of the testis architecture and echogenic lines radiate toward the mediastinum

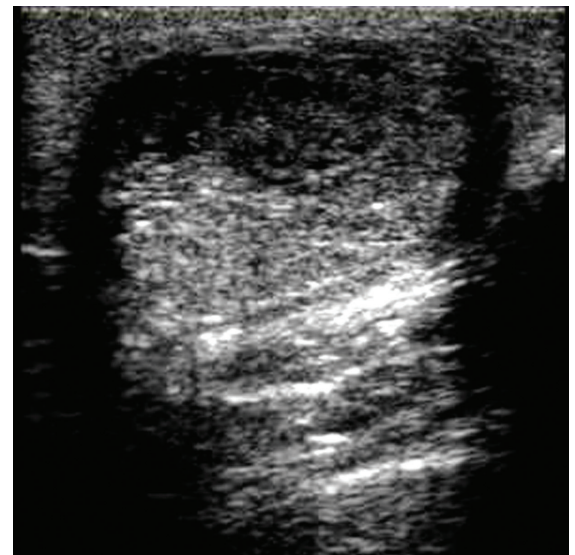


Fig 23: B-mode ultrasound image (longitudinal plane) of the testis of a six-year-old rottweiler with orchitis. There is a diffuse hypoechoic pattern evident (predominantly within the testicular parenchyma in the near field) and a thin, hypoechoic rim (presumably fluid) surrounding the testis

gradually decreases (often to half the normal volume for the breed) and the parenchyma becomes hypoechoic.

Torsion of the spermatic cord

Torsion of the spermatic cord (often called testicular torsion) commonly results in significant testicular enlargement and can be diagnosed by B-mode ultrasonography, although Doppler ultrasonography is more specific because it allows documentation of testicular artery blood flow. B-mode ultrasonography is often used to clarify the differential diagnosis of other causes of scrotal enlargement, such as scrotal hernia.

Early changes resulting from testicular torsion include enlargement of the epididymis and the presence of hydrocoele, which is a non-specific finding and may be mistaken for epididymitis. Other findings include enlargement of the spermatic cord, testicular enlargement and decreased parenchymal echogenicity (Fig 25). In the subacute phase (up to 10 days after the torsion), there may be more distinct signs including loss of normal architecture and mixed echogenicity of the affected testicle.

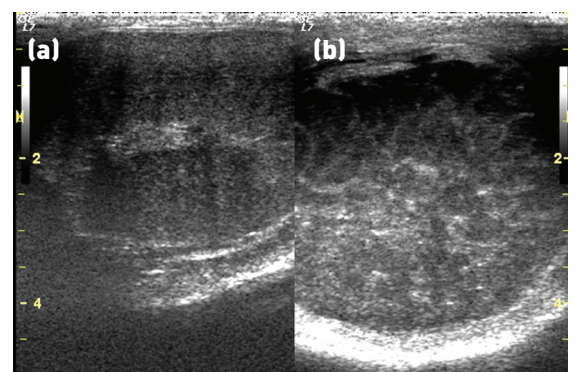
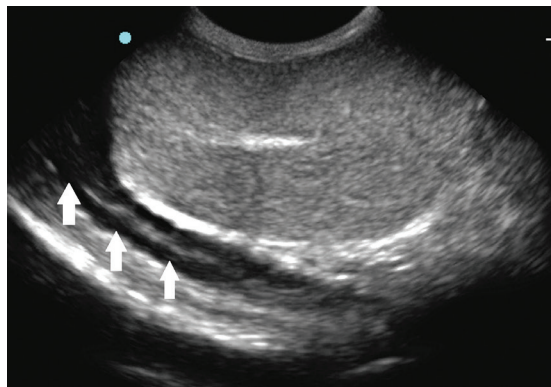


Fig 25: B-mode ultrasound image of (a) a normal testis (longitudinal plane) and (b) the contralateral testis with torsion of the spermatic cord (transverse plane). A combination of decreased background echogenicity with scattered hyperechoic regions can be seen in image of the abnormal testis

Companion Animals

Fig 26: B-mode ultrasound image (longitudinal plane) of the testis and epididymis of a six-year-old vasectomised dog. The epididymis, which runs along the border of the testis, is enlarged and has multiple tubular anechoic regions (arrows) that represent the distended epididymal lumen



Abnormalities of the epididymis

Epididymal lesions may be difficult to assess clinically; however, ultrasound evaluation allows the detection of lesions that cannot be palpated, including those that occur as a result of inflammatory disease and spermatic cord torsion. In both cases, the dimensions of the epididymis increase and there are changes in echogenicity.

Fluid-distended and enlarged epididymides may also occur in dogs that have been vasectomised (Fig 26).

Undescended testes

Undescended testes have a similar ultrasonographic appearance to normal testes, although they are usually small and hypoechoic. A characteristic feature is the longitudinal mediastinum testes. Ultrasound examination may confirm the presence of undescended testes and document the precise location with high accuracy (Felumlee and others 2012), as well as identifying torsion and neoplasia.

Doppler ultrasonography

The testis and epididymis are supplied with blood from the testicular artery. The arterial segment within the

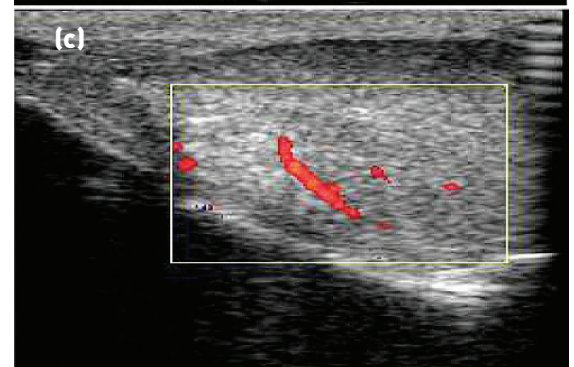
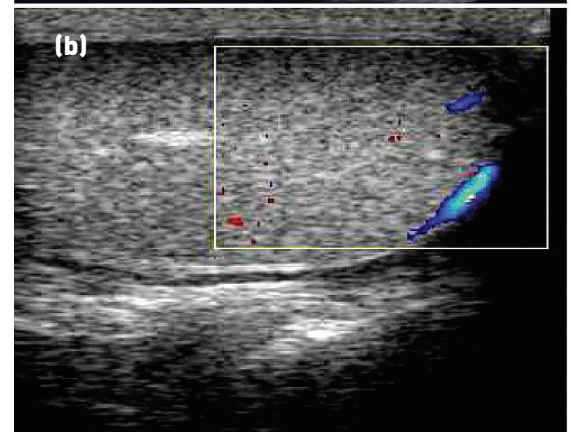
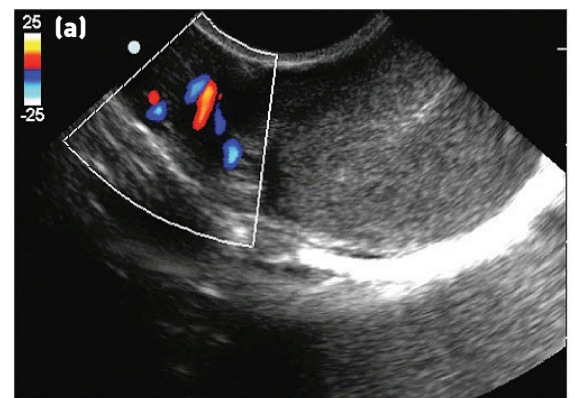


Fig 27: Colour Doppler ultrasound images of the testicular artery in (a) the suprastesticular, (b) marginal and (c) intratesticular regions

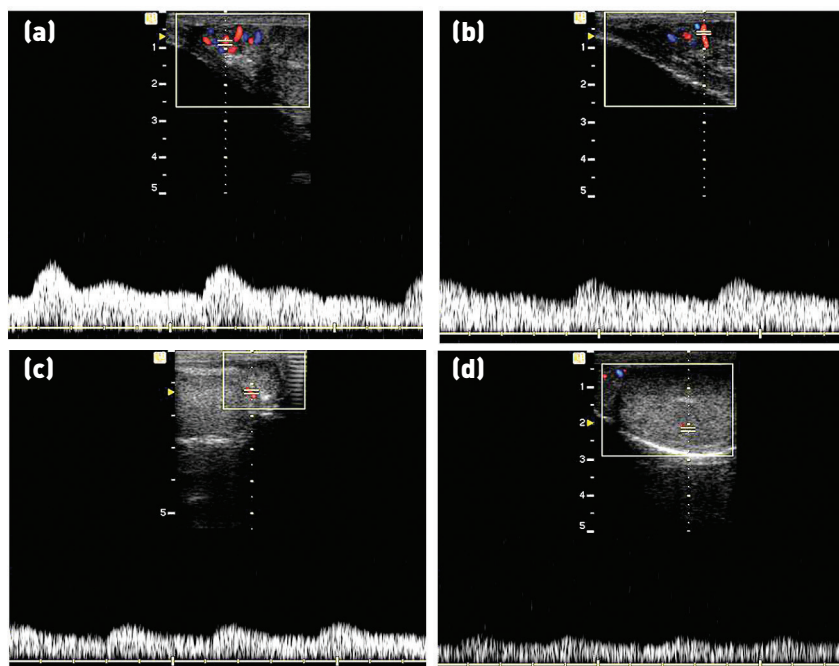


Fig 28: Pulsed-wave Doppler ultrasound images of different regions of the testicular artery. (a) Biphasic and (b) monophasic waveforms may be observed in the suprastesticular artery, whereas (c) the marginal and (d) the intratesticular regions of the artery show a monophasic flow pattern

spermatic cord has a thick wall and small lumen to allow for stretching; this section is often convoluted and is termed the suprastesticular artery (Fig 27a). The testicular artery that emerges from the spermatic cord has a thinner wall and larger lumen, and extends through the epididymal margin of the testes, near the capsule, generally running with a linear course without any branches; this is termed the marginal artery (Fig 27b). The terminal segment penetrates the testicular parenchyma, and the intratesticular arteries are directed toward the mediastinum (Fig 27c).

Centripetal arteries within the testicular parenchyma and their recurrent rami may be identified using colour-Doppler ultrasonography in oblique planes to the standard longitudinal and transverse planes.

Normal testicular arterial blood supply

Characteristics of blood flow within the testicular artery assessed by PW Doppler ultrasonography change depending upon the segment that is assessed (Fig 28). In the suprastesticular region, two waveform patterns

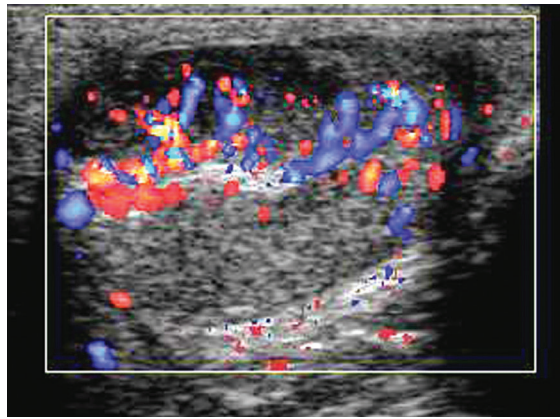


Fig 29: Power Doppler ultrasound image (longitudinal plane) of the testis of a dog with orchitis, showing increased blood flow within the testicular parenchyma

may be visualised due to the tortuous characteristic of the artery in this region: first, a biphasic waveform, with a diastolic notch followed by a diastolic peak; secondly, a monophasic waveform, characterised by a slow systolic increase followed by a decreased diastolic flow. The marginal and intratesticular regions of the artery have a low resistance flow with monophasic waveforms; this pattern is typically seen in arteries that irrigate parenchymal structures.

The PW Doppler parameters PSV, EDV, RI and PI show differences according to the region of the artery that are measured. High velocities are present within the supratesticular region, which decrease through the marginal and intratesticular regions. Also, these parameters are different in postpubertal and prepubertal dogs (de Souza and others 2015) and in dogs of different sizes (Souza and others 2014).

A relationship between PW Doppler measurements and semen quality may also be observed: lower values of PSV (eg, less than 14.0 cm/second) and higher values of RI and PI (eg, greater than 0.66 and 1.00, respectively) are associated with poor semen quality (Zelli and others 2013).

Abnormal testicular arterial blood supply

There are only a few descriptions of testicular blood flow in abnormal testes.

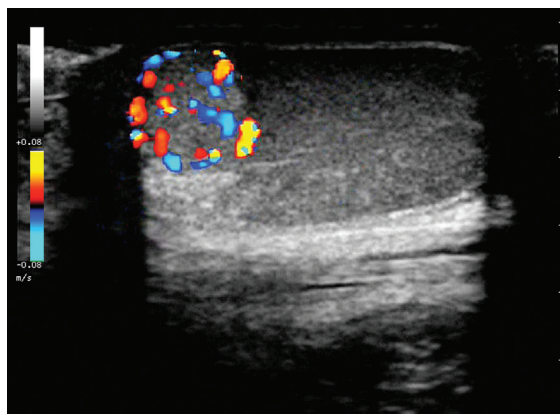


Fig 31: Colour Doppler ultrasound image (longitudinal plane) of a testis containing a focal neoplasm, showing increased blood flow within and around the tumour

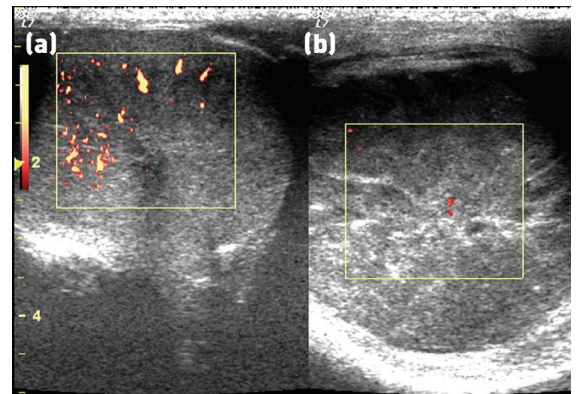


Fig 30: Power Doppler ultrasound image of (a) a testis with normal vascular perfusion and (b) the contralateral testis with torsion of the spermatic cord. There is an absence of perfusion in the image of the abnormal testis

Orchitis

In cases of orchitis, testicular artery blood flow has been shown to increase and this is associated with an increase in RI and PI values within the testicular parenchyma. Colour Doppler ultrasonography may demonstrate increased testicular parenchymal perfusion (Fig 29).

Torsion of the spermatic cord

Torsion of the spermatic cord is most common in undescended testes, often when there is testicular neoplasia, but may occur in young active males with scrotal testes. Doppler ultrasonography in the latter cases shows an absence of blood flow to and within the affected testis (Fig 30). In cases of an incomplete torsion, it may be possible to observe reduced rather than absent perfusion.

Neoplasia

There is no information about testicular arterial flow in cases of testicular neoplasia; however, colour Doppler ultrasonography shows an increase in blood flow within and around most tumours (Fig 31). While this is useful for tumour detection, the changes noted are not specific for tumour type.

Contrast-enhanced ultrasonography

Reports on the use of CEUS to evaluate the testes are scarce. However, the possibilities of using this technique are promising. As it is sensitive to changes in microvascularisation within the testes, it enables exceptional visualisation of testicular lesions and may potentially provide a better classification of lesions than that obtained using B-mode and colour Doppler ultrasonography.

Normal testes

CEUS offers advantages over Doppler ultrasonography in that testicular artery branches and parenchymal perfusion are readily observed and can be measured using quantitative methods.

After injection of the contrast agent, the tortuous supratesticular arteries become opaque, which is followed by clear highlighting of the marginal arteries and finally the intratesticular arteries, with flow directed towards the mediastinum testis. The testicular parenchyma has increased echogenicity during the vascular bed phase and then the contrast material is gradually cleared from the parenchyma during the wash-out phase.

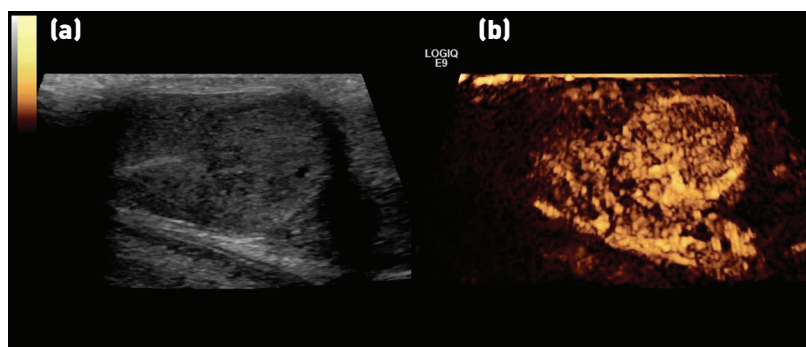


Fig 32: (a) B-mode and (b) contrast-enhanced ultrasound images of the testis of a dog with an interstitial cell tumour. There is a poorly demarcated focal lesion that is difficult to appreciate on the B-mode image, but it has a marked enhanced appearance after the injection of the contrast material

Testicular veins are highlighted but are of lower echogenicity compared to the arteries because persistence within the vascular bed results in a longer wash-out than wash-in period.

Reliable data have been provided for the use of CEUS in normal dogs using standard protocols for administration of the contrast agent (Volta and others 2014); however, limitations include the high costs of the contrast material and the need for specialised ultrasound equipment. Quantitative measurements for normal testes in anaesthetised dogs show a wash-in phase of approximately 27 seconds, mean peak perfusion intensity of 16.6 per cent, time to reach peak intensity of 35 seconds and a wash-out phase of 40 seconds. Further studies are needed to document variations in perfusion kinetics and to establish more rapid protocols that can be applied to conscious dogs.

Abnormal testes

Normal testes are characterised by a homogeneous, moderately enhanced parenchyma during the rapid wash-in phase. Generally, non-neoplastic lesions (eg, chronic orchitis, degeneration or atrophy) show a homogeneous pattern, with lower enhancement than that in non-pathological tissue. Neoplastic lesions (eg, seminomas, Sertoli cell tumours) have a heterogeneous appearance with a hyperenhanced pattern and persistent inner vessels (Fig 32).

New techniques

Recent studies in human medicine have reported that acoustic radiation force impulse elastography can be useful for the evaluation of the prostate gland and testes. With this method, the velocity of propagation and attenuation of ultrasound waves are related to the rigidity and viscoelasticity of tissues, such that the subtle changes in tissue properties that occur with some disease conditions may be detected. Feliciano and others (2015) have established reference values for the prostate gland and testes of normal dogs but, at the time of writing, no clinical diagnostic studies have been performed.

Conclusion

Although B-mode imaging of the prostate gland and testes of the dog has been undertaken clinically for more than 30 years, there has been substantial improvement in ultrasound equipment technology, and recent studies

of arterial blood flow and vascularisation using Doppler ultrasonography and CEUS have added to the knowledge base. There is no doubt that these advanced ultrasound techniques are now increasingly common as diagnostic tools for the investigation of canine prostatic and testicular diseases.

References

- ATALAN, G., HOLT, P. E., BARR, F. J. & BROWN, P. J. (1999) Ultrasonographic estimation of prostate size in canine cadavers. *Research in Veterinary Science* **67**, 7-15
- BIGLIARDI, E. & FERRARI, L. (2011) Contrast-enhanced ultrasound of the normal canine prostate gland. *Veterinary Radiology and Ultrasound* **52**, 107-110
- DE SOUZA, M. B., BARBOSA, C. C., ENGLAND, G. C., MOTA FILHO, A. C., SOUSA, C. V., DE CARVALHO, G. G. & OTHERS (2015) Regional differences of testicular artery blood flow in post pubertal and pre-pubertal dogs. *BMC Veterinary Research* **11**, 47
- FELICIANO, M. A., MARONEZI, M. C., SIMÕES, A. P., USCATEGUI, R. R., MACIEL, G. S., CARVALHO, C. F. & OTHERS (2015) Acoustic radiation force impulse elastography of prostate and testes of healthy dogs: preliminary results. *Journal of Small Animal Practice* **56**, 320-324
- FELUMLEE, A. E., REICHLER, J. K., HECHT, S., PENNINGCK, D., ZEKAS, L., DIETZE YEAGER, A. & OTHERS (2012) Use of ultrasound to locate retained testes in dogs and cats. *Veterinary Radiology and Ultrasound* **53**, 581-585
- FREITAS, L. A., PINTO, J. N., SILVA, H. V. & DA SILVA, L. D. (2015) Two-dimensional and Doppler sonographic prostatic appearance of sexually intact French bulldogs. *Theriogenology* **83**, 1140-1146
- MANTZIARAS, G., ALONGE, S. & LUVONI, G. C. (2014) Ultrasonographic study of age-related changes on the size of prostate and testicles in healthy German shepherd dogs. Seventeenth European Veterinary Society for Small Animal Reproduction Congress. Wroclaw, Poland, September 26, 2014. p 150
- PUGH, C. R., KONDE, L. J. & PARK, R. D. (1990) Testicular ultrasound in the normal dog. *Veterinary Radiology and Ultrasound* **31**, 195-199
- RUSSO, M., VIGNOLI, M., CATONE, G., ROSSI, F., ATTANASI, G. & ENGLAND, G. C. (2009) Prostatic perfusion in the dog using contrast-enhanced Doppler ultrasound. *Reproduction in Domestic Animals* **44** (Suppl 2), 334-335
- RUSSO, M., VIGNOLI, M. & ENGLAND, G. C. (2012) B-mode and contrast-enhanced ultrasonographic findings in canine prostatic disorders. *Reproduction in Domestic Animals* **47** (Suppl 6), 238-242
- SOUZA, M. B., MOTA FILHO, A. C., SOUSA, C. V. S., MONTEIRO, C. L. B., CARVALHO, G. G., PINTO, J. N. & OTHERS (2014) Triplex Doppler evaluation of the testes in dogs of different sizes. *Pesquisa Veterinária Brasileira* **34**, 1135-1140
- VIGNOLI, M., RUSSO, M., CATONE, G., ROSSI, F., ATTANASI, G., TERRAGNI, R. & OTHERS (2011) Assessment of vascular perfusion kinetics using contrast-enhanced ultrasound for the diagnosis of prostatic disease in dogs. *Reproduction in Domestic Animals* **46**, 209-213
- VOLTA, A., MANFREDI, S., VIGNOLI, M., RUSSO, M., ENGLAND, G. C., ROSSI, F. & OTHERS (2014) Use of contrast-enhanced ultrasonography in chronic pathologic canine testes. *Reproduction in Domestic Animals* **49**, 202-209
- ZELLI, R., TROISI, A., ELAD NGNONPUT, A., CARDINALI, L. & POLISCA, A. (2013) Evaluation of testicular artery blood flow by Doppler ultrasonography as a predictor of spermatogenesis in the dog. *Research in Veterinary Science* **95**, 632-637
- Further reading**
- ENGLAND, G. C. W. (1991) The relationship between ultrasonographic appearance, testicular size, spermatozoal output and testicular lesions in the dog. *Journal of Small Animal Practice* **32**, 306-311
- ENGLAND, G. C. W. (1995) Ultrasonographic diagnosis of non-palpable Sertoli cell tumours in infertile dogs. *Journal of Small Animal Practice* **36**, 476-480

Ultrasonography of the prostate gland and testes in dogs

Mírley Barbosa de Souza, Lúcia Daniel Machado da Silva, Rachel Moxon, Marco Russo and Gary C. W. England

In Practice published online December 30, 2016

Updated information and services can be found at:
<http://inpractice.bmj.com/content/early/2016/12/30/inp.i6054>

These include:

References

This article cites 15 articles, 0 of which you can access for free at:
<http://inpractice.bmj.com/content/early/2016/12/30/inp.i6054#BIBL>

Email alerting service

Receive free email alerts when new articles cite this article. Sign up in the box at the top right corner of the online article.

Notes

To request permissions go to:
<http://group.bmj.com/group/rights-licensing/permissions>

To order reprints go to:
<http://journals.bmj.com/cgi/reprintform>

To subscribe to BMJ go to:
<http://group.bmj.com/subscribe/>